SCIENTIFIC REPORTS

OPEN

SUBJECT AREAS:
MAGNETIC PROPERTIES AND MATERIALS
ELECTRONIC PROPERTIES AND MATERIALS

Received
1 September 2014

Accepted
20 October 2014

Published
11 November 2014

Correspondence and requests for materials should be addressed to D.H.W. (wangdh@nju.edu.cn)

Electric field manipulation of magnetic and transport properties in $SrRuO_3$/$Pb(Mg_{1/3}Nb_{2/3})O_3$-$PbTiO_3$ heterostructure

W. P. Zhou, Q. Li, Y. Q. Xiong, Q. M. Zhang, D. H. Wang, Q. Q. Cao, L. Y. Lv & Y. W. Du

Jiangsu Key Laboratory for Nano Technology and National Laboratory of Solid State Microstructures, Nanjing University, Nanjing 210093, People's Republic of China.

The electric field manipulation of magnetic properties is currently of great interest for the opportunities provided in low-energy-consuming spintronics devices. Here, we report the effect of electric field on magnetic and transport properties of the ferromagnetic $SrRuO_3$ film which is epitaxially grown on $Pb(Mg_{1/3}Nb_{2/3})O_3$-$PbTiO_3$ ferroelectric substrate. With the application of electric field on the substrate, the magnetization, Curie temperature and resistivity of $SrRuO_3$ are effectively modified. The mechanism of the electric field manipulation of these properties is ascribed to the rotations of RuO_6 oxygen octahedra caused by the electric-field-induced strain, which changes the overlap and hybridization between the Ru 4*d* orbitals and O 2*p* orbitals, resulting in the modification of the magnetic and electronic properties.

Magnetoelectric (ME) heterostructures consisting of ferromagnetic and ferroelectric elements have aroused great interest in recent years for their rich coupling mechanisms and promising applications in next-generation electronic devices[1–6]. The ME effects can be classified as direct ME (DME) and converse ME (CME), which are characterized as magnetic-field-induced polarization and electric-field-induced magnetization, respectively. The CME effect, i.e. electric field control of magnetism, is now a research focus, since it can provide a low-consuming method to manipulate the magnetization[1,3,4]. Up to now, the most used CME mode is the strain-mediated coupling[1,7]. By depositing the ferromagnetic component on ferroelectric/piezoelectric substrate, the electric-field-induced strain can remarkably manipulate magnetization, giving rise to large ME effects[8–10]. $Pb(Mg_{1/3}Nb_{2/3})O_3$–$PbTiO_3$(PMN-PT) and $PbZr_xTi_{1-x}O_3$(PZT) are frequently selected as the ferroelectric/piezoelectric substrates due to their excellent piezoelectric and ferroelectric performance. As for the ferromagnetic components, magnetic perovskites are ideal candidates because they exhibit abundant physical properties and are easy to grow epitaxially on the ferroelectric substrates[10–13]. In magnetic-perovskite-based ME heterostructures, the magnetism can be manipulated by means of altering the magnetic anisotropy[10], affecting the phase separation[11,12], or adjusting the spin state of magnetic ions[13] through the electric-field-induced strain. In addition to strain-mediated mechanism, ferroelectric field-effect[14] may also plays a role in tuning magnetic and transport properties of magnetic perovskites in those ME heterostructures due to the accumulation or depletion of charge carries at interface through ferroelectric polarization reversal[15–17]. It is known that networks of corner-sharing oxygen octahedra play an important role in determining the magnetic and electronic properties of the perovskite through its deformations, rotations or tilts[18–20]. Recently, theoretical results based on the first-principles calculation point out that the magnetization can be controlled via octahedral rotations in a perovskite related oxide[21]. Since the oxygen octahedral rotations in perovskites can be manipulated by applying stress[18], it may provide an opportunity to achieve CME effect in magnetic perovskites.

$SrRuO_3$ (SRO) is a moderately correlated material and the only known *4d* transition metal oxide with ferromagnetic order and metallic behavior, which has attracted an enormous amount of investigation for its intriguing magnetic and electronic properties[22]. The perovskite structure of SRO crystallizes in orthorhombic symmetry, exhibiting a $GdFeO_3$-kind of distortion associated with rotation and tilt of RuO_6 octahedra[22]. The manipulation of resistivity by ferroelectric field-effect has been reported in a SRO/PZT heterostructure, in which a 9% change of the resistivity upon reversing the ferroelectric polarization is observed[23]. However, there are few reports about the electric-field control of magnetization or resistivity in SRO film using strain-mediated

mechanism. As we know, density-functional theory calculations have predicted that the magnetic moment is suppressed under compressive strain and enhanced with tensile strain for (001)-epitaxial SRO films due to the strain-induced oxygen octahedral rotations[24]. As for the experimental results, Gan *et.al* reported that, compared with the strain relaxed film, the saturation magnetic moment can be suppressed in the compressive SRO film[25]. Moreover, Terai *et.al* found that the Curie temperature (T_C) of SRO is enhanced under tensile strain[26]. Up to now, most of the studies about the strain dependent of magnetic properties for SRO are focused on the films deposited on various substrates, in which the different strain states are attributed to the mismatch of lattice parameters[27–29]. Since the magnetic properties of these films are entangled with other factors such as non-stoichiometry, defects, impurities, interdiffusion with the substrate or surface morphology, it is not strict to isolate strain effects by comparing with each other[22,30]. However, depositing SRO film on the piezoelectric substrate can neglect these intricacies and provide an electric-field-controlled strain state *in-situ*, which is helpful to gain more insight on the strain impact on the magnetic properties of the film. In this paper, we deposit SRO film on PMN-PT substrate and investigate the electric field manipulation of magnetization and resistivity by applying an electric field on the piezoelectric single crystal. The experimental results show that not only the saturation magnetization but also T_C can be affected by the electric field, showing an intrinsic CME effect. The effect of electric field on the resistivity further demonstrates the correlation between magnetic and electric properties of SRO film.

Results

The XRD θ-2θ scan of SRO/PMN-PT heterostructure is shown in Fig. 1(a). Obviously, only the diffraction peaks of substrate and film can be observed, suggesting the single phase and highly (001)-oriented nature of the film. Although the structure of PMN-PT crystal and bulk SRO are rhombohedral and orthorhombic respectively, they can be regarded as the pseudocubic structures with lattice parameters of $a_{\text{PMN-PT}}$=4.02 Å and a_{SRO}=3.93 Å. Due to the lattice mismatch (~2.3%) between SRO and PMN-PT, the SRO film is under the substrate-induced tensile strain along the in-plane direction. Besides the epitaxial growth, the surface morphology of the film is also important for the efficiency of strain transferred from the substrate to the film in strain-mediated ME heterostructures[17]. The AFM image exhibited in Fig. 1(b) with an area of 2 × 2 μm^2 shows a rather smooth surface with the root mean square roughness about 0.4 nm. Therefore, the structural and morphological features of SRO film demonstrate a favorable condition for the following CME coupling measurements.

For investigating the effect of electric field on the magnetism, we measure the thermomagnetic curves for SRO film with or without electric field, where the applying magnetic field and electric field are 500 Oe and 8 kV/cm, respectively. As shown in Fig. 2, SRO film shows a typical ferromagnetic transition and the value of T_C under zero electric field is around 117 K. With the application of electric field, an obvious suppression of the magnetization and a shift of T_C are observed simultaneously. The upper inset of Fig. 2 shows the temperature dependence of the relative change of magnetization $\Delta M/M$ ($\Delta M/M = [M(E) - M(0)]/M(0)$, where $M(E)$ and $M(0)$ are the magnetization with and without electric field, respectively.). A negative CME effect with a peak value of −26.8% near 117 K is observed in SRO film by applying an electric field on the PMN-PT substrate. To further determine the variation of T_C caused by the electric field, we extract T_C from extrapolating the linear part of M^2-T curve to M=0 in a temperature range below T_C[31]. As shown in the bottom inset of Fig. 2, T_C shifts from 117 K to 115 K with an electric field of 8 kV/cm. According to the earlier reports[8-10], the magnetization of the strain-mediated ME system is usually modified by altering the magnetic anisotropy, giving rise to an extrinsic CME effect. However, in the case of SRO/PMN-PT heterostructure, not only the magnetization but also T_C varies with the electric field, suggesting that the CME effect in SRO film may have other coupling mechanism.

Figure 3 shows the magnetic hysteresis loops (M-H) at 115 K under the electric fields of zero and 12 kV/cm with the magnetic field parallel to the film surface, and the schematic diagram of laminate structure and magnetic measurement is shown in the inset. It is obvious that both M-H curves show typical ferromagnetic character and are almost saturated under the magnetic field of 5 kOe. With the application of electric field, a noticeable separation of magnetization can be observed. The value of $\Delta M/M$ under the magnetic field of 5 kOe is about −8.6%. As we know, the modification of magnetic anisotropy can affect the magnetization, but cannot change the saturation magnetization. Therefore, the electric field would have an intrinsic effect on the magnetism of SRO film due to the change of saturation magnetization.

To further explore the origin of electric field control of magnetism in SRO/PMN-PT heterostructure, the relative change of magnetization $\Delta M/M$ as a function of bipolar electric field with a bias magnetic field of 500 Oe is measured at 115 K. As shown in Fig. 4(a), a hysteresis loop with a rather symmetric butterfly shape is observed, which is consistent with the shape of strain vs electric field hysteresis loop and different from that of polarization vs electric field hysteresis loop of the PMN-PT substrate[17]. Thus the observed electric field manipulation of magnetization in SRO/PMN-PT heterostructure

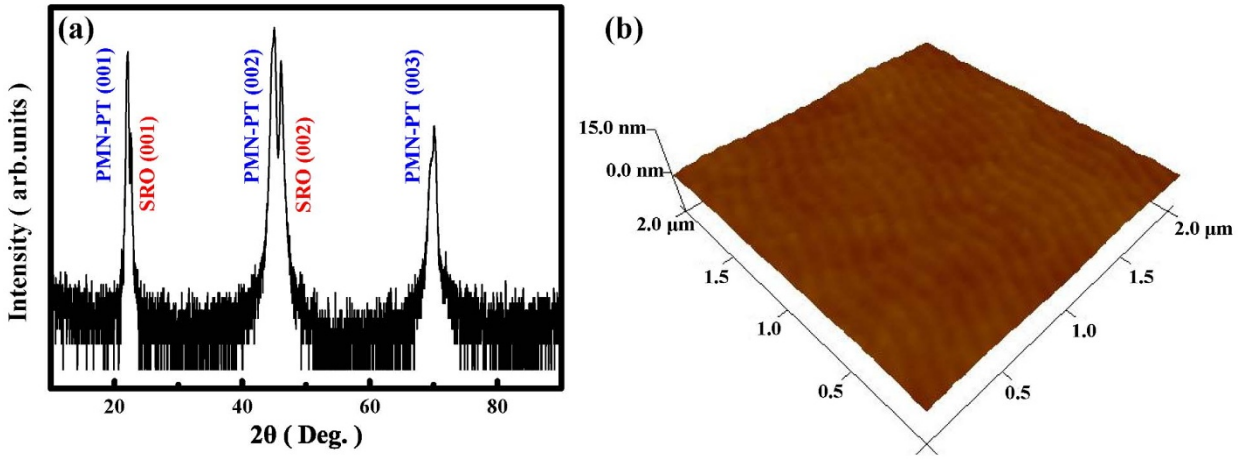

Figure 1 | (a) XRD pattern for SRO/PMN-PT heterostructure at room temperature. (b) Surface morphology of SRO film with an area of 2 × 2 μm^2.

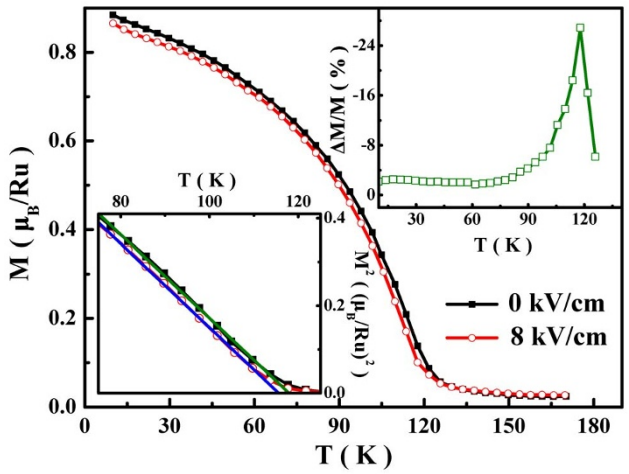

Figure 2 | The temperature dependence of magnetization *M*-*T* curves for SRO/PMN-PT heterostructure under 500 Oe with electric fields of 0 and 8 kV/cm. The upper inset is the relative change of magnetization $\Delta M/M$. The bottom inset is M^2-T curves under 0 and 8 kV/cm with straight lines fitted to determining T_C.

would be ascribed to the electric-field-induced strain. When an electric field is applied on PMN-PT with the direction parallel to the polarization, the substrate would contract along the in-plane direction which causes the reduction of magnetization of the upper SRO layer about 9.2% under an electric field of 20 kV/cm. As the electric field reverse its direction, a tensile strain is produced, which leads to the enhancement of magnetization with a maximum value of about 6.7% at the coercivity field of 10.8 kV/cm. Compared with the earlier report about depositing SRO film on different substrates[29], this method of controlling magnetism in SRO is adjustable and scalable, since the applying electric field can be continuously tuned and the value of generated stress is also countable[32]. After the substrate is poled with a positive electric field, the time dependence of magnetization and electric field is measured with a bias magnetic field of 500 Oe. As shown in Fig. 4(b), when an electric field of 12 kV/cm is applied, SRO film exhibits a low magnetization state of 0.139 μ_B/Ru. While the electric field turns off, it subsequently transforms into a high magnetization state of 0.149 μ_B/Ru. Furthermore, the magnetization of SRO film shows almost stable change after several cycles with the electric field switching on and off alternatively, suggesting

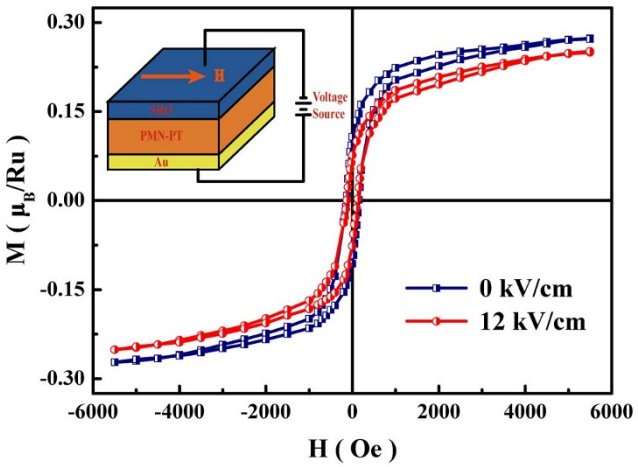

Figure 3 | *M*-*H* loops for SRO/PMN-PT heterostructure measured under electric fields of 0 and 12 kV/cm at 115 K. The inset shows the schematic diagram of the laminate structure and magnetic measurements, where magnetic field is applied parallel to the film surface.

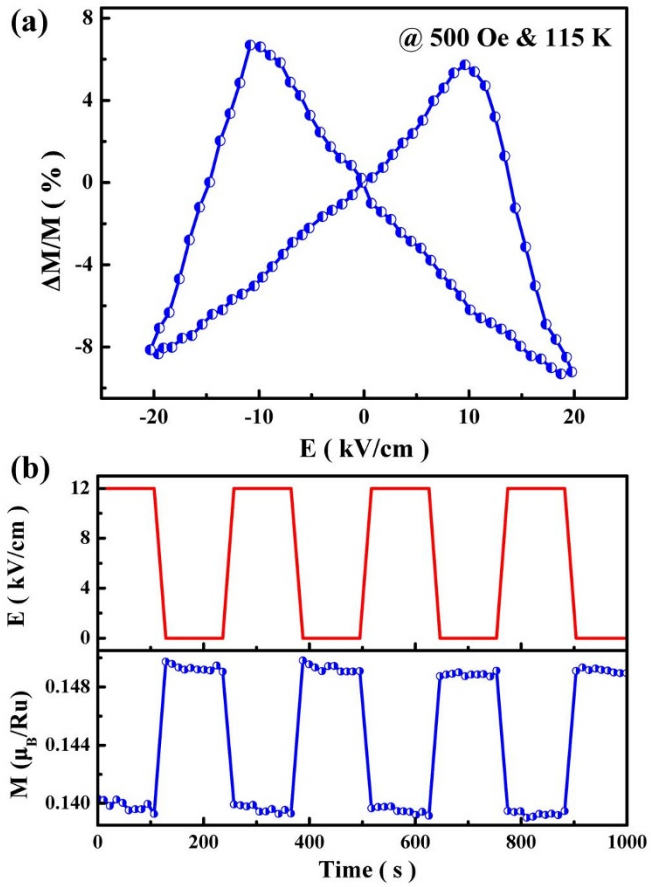

Figure 4 | (a) The hysteresis loop of $\Delta M/M$ as a function of bipolar electric field for SRO film at 115 K with a bias magnetic field of 500 Oe. (b) The variation of electric field and magnetization as a function of time with a bias magnetic field of 500 Oe at 115 K.

that the magnetization of this heterostructure can be reversibly and reproducibly controlled by the electric field.

As mentioned above, SRO is a kind of moderately correlated material, in which the transport and magnetism are related with the conduction *d* band, leading to an intrinsic coupling between the magnetic and transport properties[22]. Therefore, the electric field would have influence on the transport properties of SRO film as well. Figure 5(a) shows the temperature dependence of resistivity for SRO film with and without electric fields, and the schematic image of electric measurement is shown in the inset. Under zero electric field, the resistivity decreases almost linearly with the temperature cooling down from room temperature, exhibiting a typical behavior of "bad metal"[33]. When the temperature further decreases, a kink is observed around T_C and the resistivity decreases rapidly below this temperature due to the loss of spin disorder scattering[34]. It is obvious that the resistivity of SRO film decreases in the measured temperature regions with the application of an electric field on PMN-PT substrate. We also measure the hysteresis loop of the relative change of resistivity $\Delta R/R$ ($\Delta R/R = [R(E) - R(0)]/R(0)$) as a function of bipolar electric field at 115 K. As demonstrated in Fig. 5(b), $\Delta R/R$ exhibits a nearly symmetric butterfly shape with the variation of electric field, which is similar with the $\Delta M/M$ -*E* hysteresis loop, further suggesting that the electric field modulation of the resistivity stems from the electric-field-induced strain as well. Under the compressive strain, the resistivity of SRO film decreases about 1.3% at an electric field of 20 kV/cm. While the tensile strain is found to increase the resistivity with a maximum value about 1.1% at the coercivity field of 10 kV/cm. The resistivity response to the variation

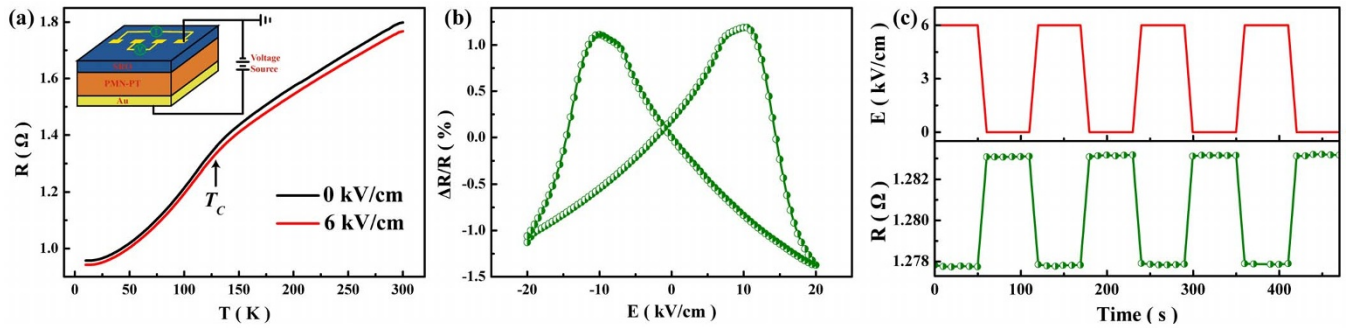

Figure 5 | (a) The temperature dependence of *R-T* curves for SRO/PMN-PT heterostructure with electric fields of 0 and 6 kV/cm. The inset shows the schematic diagram of device configuration for resistivity measurements. (b) The hysteresis loop of $\Delta R/R$ as a function of bipolar electric field for SRO film at 115 K. (c) The resistivity response to the variation of electric field as a function of time for SRO film measured at 115 K.

of electric field as a function of time for SRO film is also measured at 115 K with the substrate poled under a positive electric field. As shown in Fig. 5 (c), the resistivity reduces with the electric field switching on and restores its initial state immediately with the electric field switching off, showing a same behavior with that of magnetization. The reversible modulation of the resistivity $\Delta R/R$ is about −0.5% with an applied field of 6 kV/cm.

Discussion

It is well accepted that there is a rather strong hybridization between the Ru 4*d* orbitals and O 2*p* orbitals of SRO, leading to a ferromagnetic ground state[35,36]. However, in the case of $CaRuO_3$, it possesses the same structure as that of $SrRuO_3$, but has larger rotations of the RO_6 oxygen octahedra, which results in a paramagnetic ground state[37]. This fact suggests that the octahedral rotations and tilts play a key role in determining the magnetic state of $ARuO_3$ (A=Ca, Sr) system and the magnetic properties of them can be adjusted through modulation of the hybridization between the Ru 4*d* and O 2*p* states by structural distortions[19]. In SRO/PMN-PT heterostructure, when an electric field is applied with the direction parallel to the polarization, the PMN-PT substrate would contract along in-plane direction and weaken the as-grown tensile strain. As illustrated in Fig. 6, in order to adapt this contraction, the RuO_6 octahedral rotation angle of SRO film would enlarge correspondingly, giving rise to the enhancement of the overlap and hybridization between the Ru 4*d* orbitals and O 2*p* orbitals[18,19,38]. Therefore, the magnetic interaction would reduce[36,39], which leads to the decrease of magnetization and T_C, showing an intrinsic CME effect.

Since the strain, $\Delta M/M$ and $\Delta R/R$ have the similar electric-field dependence, we can assume that the magnetization and resistivity change linearly with the strain. When an electric field of 8 kV/cm is applied, an in-plane compression of about 0.1% is generated[11], leading to the decrease of T_C of SRO film for about 2 K, as shown in Fig. 2. This result is comparable with that reported by Terai *et.al*[26], where the strain of 0.25% results in the variation of T_C for about 4 K for SRO film grown on $Ba_{1-x}Sr_xTiO_3/BaTiO_3$ buffer layers. As for the magnetization, the saturation magnetization of SRO film decreases about 8.6% near T_C under an electric field of 12 kV/cm (about 0.12% compressive strain[32]), corresponding to about 71.7% reduction of magnetization under 1% compressive strain. This result is dramatically larger than that reported by Gan *et.al*[25], in which the saturation magnetization of SRO decreases about 20% under a 0.67% compressive strain at 10 K. The larger effect of elastic strain on saturation magnetization in our sample reflects that the magnetism of SRO film responds more sensitive to the strain near T_C, as revealed in the upper inset of Fig. 2.

The electric field manipulation of resistivity can also be attributed to the oxygen octahedral rotations caused by the strain. In order to accommodate the electric-field-induced strain, the Ru-O-Ru bond angles, which is determined by the rotation of the oxygen octahedra, would change and the overlap between the Ru 4*d* states and O 2*p* states would enhance correspondingly[18,40]. As a result, the variation of the Ru-O-Ru bond angles affects the electron hopping matrix elements while the enhanced orbital overlap broadens the electron bandwidth and reduces the correlation effect, leading to the decrease of resistivity[36,40,41].

In conclusion, the electric field control of magnetic and transport properties of SRO/PMN-PT heterostructure have been investigated. We demonstrate that the saturation magnetization, T_C, and resistivity of SRO film can be manipulated with the application of electric field. Moreover, the magnetization and resistivity can be controlled reversibly and reproducibly with *in situ* electric field. The observed CME effect in SRO/PMN-PT heterostructure can be understood in the scenario of electric-field-induce strain modulates the hybridization between the Ru 4*d* orbitals and O 2*p* orbitals through altering the octahedral rotations. This result suggests an alternative mechanism for intrinsic CME effect in perovskite films through controlling octahedral rotations. The electric field control of magnetic and transport properties in SRO/PMN-PT heterostructure provide a potential application in low-energy-consuming spintronics devices.

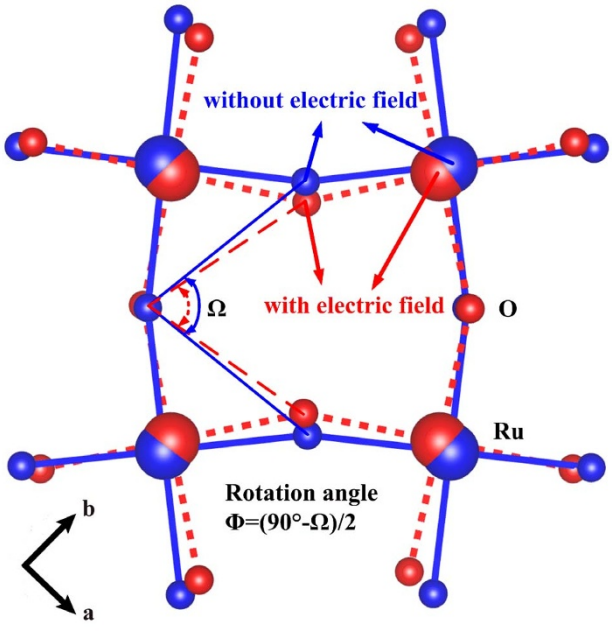

Figure 6 | **Illustration of RuO_6 octahedral rotations with (red color) and without (blue color) electric field, where the rotation angle can be defined as (90°-Ω)/2.** (Large circles represent Ru atoms while small circles represent O atoms.)

Methods

SRO film with thickness about 300 nm was deposited on polished (001)-oriented PMN-PT substrate with dimensions of $5 \times 5 \times 0.5$ mm^3 by pulsed laser deposition method with a 248 nm KrF excimer laser. During the growth, the substrate temperature was 700°C and the background oxygen pressure was 13 Pa. After deposition, the film was cooled down in oxygen of 2×10^4 Pa. X-ray diffraction (XRD) and atomic force microscopy (AFM) measurements were performed to characterize the structure and surface topography of the film. To conduct the investigation of electric field on magnetic and transport properties *in situ*, Au layer was sputtered on the backside of the PMN-PT substrate as bottom electrode while the conducting SRO layer acts as top electrode. The PMN-PT substrate was poled at 350 K under an electric field of 8 kV/cm for 30 min. before measuring the CME effect. The magnetic properties were measured with a magnetic property measurement system (MPMS, Quantum Design) and the transport properties were measured by four probes method with a physical property measurement system (PPMS, Quantum Design). Electric voltage was applied *in situ* by a source meter (Keithley, model 2410).

1. Ma, J., Hu, J. M., Li, Z. & Nan, C. W. Recent Progress in Multiferroic Magnetoelectric Composites: from Bulk to Thin Films. *Adv. Mater.* **23**, 1062–1087 (2011).
2. Eerenstein, W., Mathur, N. D. & Scott, J. F. Multiferroic and magnetoelectric materials. *Nature* **442**, 759–765 (2006).
3. Wu, S. *et al.* Reversible electric control of exchange bias in a multiferroic field-effect device. *Nature Mater.* **9**, 756–761 (2010).
4. Bibes, M. & Barthélémy, A. Towards a magnetoelectric memory. *Nature Mater.* **7**, 425–426 (2008).
5. Wang, Y. *et al.* An extremely low equivalent magnetic noise magnetoelectric sensor. *Adv. Mater.* **23**, 4111–4114 (2011).
6. Nan, C.-W., Bichurin, M., Dong, S., Viehland, D. & Srinivasan, G. Multiferroic magnetoelectric composites: historical perspective, status, and future directions. *J. Appl. Phys.* **103**, 031101 (2008).
7. Vaz, C. A. F. Electric field control of magnetism in multiferroic heterostructures. *J. Phys.: Condens. Matter.* **24**, 333201 (2012).
8. Liu, M. *et al.* Giant electric field tuning of magnetic properties in multiferroic ferrite/ferroelectric heterostructures. *Adv. Funct. Mater.* **19**, 1826–1831 (2009).
9. Buzzi, M. *et al.* Single domain spin manipulation by electric fields in strain coupled artificial multiferroic nanostructures. *Phys. Rev. Lett.* **111**, 027204 (2013).
10. Yang, Y. *et al.* Large anisotropic remnant magnetization tunability in (011)-$La_{2/3}Sr_{1/3}MnO_3$/0.7$Pb(Mg_{2/3}Nb_{1/3})O_3$-0.3$PbTiO_3$ multiferroic epitaxial heterostructures. *Appl. Phys. Lett.* **100**, 043506 (2012).
11. Chen, Q. *et al.* Electric-field control of phase separation and memory effect in $Pr_{0.6}Ca_{0.4}MnO_3/Pb(Mg_{1/3}Nb_{2/3})_{0.7}Ti_{0.3}O_3$ heterostructures. *Appl. Phys. Lett.* **98**, 172507 (2011).
12. Zheng, M. *et al.* Coupling of magnetic field and lattice strain and its impact on electronic phase separation in $La_{0.335}Pr_{0.335}Ca_{0.33}MnO_3$/ferroelectric crystal heterostructures. *Appl. Phys. Lett.* **103**, 263507 (2013).
13. Zhang, Q. M. *et al.* The electric field manipulation of magnetization in $La_{1-x}Sr_xCoO_3/Pb(Mg_{1/3}Nb_{2/3})O_3$-$PbTiO_3$ heterostructures. *Appl. Phys. Lett.* **104**, 142409 (2014).
14. Ahn, C. H., Triscone, J.-M. & Mannhart, J. Electric field effect in correlated oxide systems. *Nature* **424**, 1015–1018 (2003).
15. Molegraaf, H. J. A. *et al.* Magnetoelectric effects in complex oxides with competing ground states. *Adv. Mater.* **21,** 3470–3474 (2009).
16. Zhu, Q. X. *et al.* Coaction and competition between the ferroelectric field effect and the strain effect in $Pr_{0.5}Ca_{0.5}MnO_3$ film/0.67$Pb(Mg_{1/3}Nb_{2/3})O_3$-0.33$PbTiO_3$ crystal heterostructures. *Appl. Phys. Lett.* **101**, 172906 (2012).
17. Jiang, T. *et al.* Coaction and distinguishment of converse piezoelectric and field effects in $La_{0.7}Ca_{0.3}MnO_3/SrTiO_3$/0.68$Pb(Mg_{1/3}Nb_{2/3})O_3-0.32PbTiO_3$ heterostructures. *Appl. Phys. Lett.* **103**, 053504 (2013).
18. Vailionis, A. *et al.* Misfit strain accommodation in epitaxial ABO_3 perovskites: Lattice rotations and lattice modulations. *Phys. Rev. B* **83**, 064101 (2011).
19. He, J., Borisevich, A., Kalinin, S. V., Pennycook, S. J. & Pantelides, S. T. Control of octahedral tilts and magnetic properties of perovskite oxide heterostructures by substrate symmetry. *Phys. Rev. Lett.* **105**, 227203 (2010).
20. Lu, W., Yang, P., Song, W. D., Chow, G. M. & Chen, J. S. Control of oxygen octahedral rotations and physical properties in $SrRuO_3$ films. *Phys. Rev. B* **88**, 214115 (2013).
21. Benedek, N. A. & Fennie, C. J. Hybrid improper ferroelectricity: a mechanism for controllable polarization-magnetization coupling. *Phys. Rev. Lett.* **106**, 107204 (2011).
22. Koster, G. *et al.* Structure, physical properties, and applications of $SrRuO_3$ thin films. *Rev. Mod. Phys.* **84**, 253 (2012).
23. Ahn, C. H. *et al.* Ferroelectric field effect in ultrathin $SrRuO_3$ films. *Appl. Phys. Lett.* **70**, 206–208 (1997).
24. Zayak, A., Huang, X., Neaton, J. & Rabe, K. M. Structural, electronic, and magnetic properties of $SrRuO_3$ under epitaxial strain. *Phys. Rev. B* **74**, 094104 (2006).
25. Gan, Q., Rao, R., Eom, C., Garrett, J. & Lee, M. Direct measurement of strain effects on magnetic and electrical properties of epitaxial $SrRuO_3$ thin films. *Appl. Phys. Lett.* **72**, 978–980 (1998).
26. Terai, K., Ohnishi, T., Lippmaa, M., Koinuma, H. & Kawasaki, M. Magnetic properties of strain-controlled $SrRuO_3$ thin films. *Jpn. J. Appl. Phys.* **43**, L227 (2004).
27. Wang, X. *et al.* Magnetic anisotropy and transport properties of 70 nm $SrRuO_3$ films grown on different substrates. *J. Appl. Phys.* **109**, 07D707 (2011).
28. Gu, M. *et al.* Magnetic Ordering and Structural Phase Transitions in a Strained Ultrathin $SrRuO_3/SrTiO_3$ Superlattice. *Phys. Rev. Lett.* **109**, 157003 (2012).
29. Grutter, A., Wong, F., Arenholz, E., Liberati, M. & Suzuki, Y. Enhanced magnetization in epitaxial $SrRuO_3$ thin films via substrate-induced strain. *J. Appl. Phys.* **107**, 09E138 (2010).
30. Siemons, W. *et al.* Dependence of the electronic structure of $SrRuO_3$ and its degree of correlation on cation off-stoichiometry. *Phys. Rev. B* **76**, 075126 (2007).
31. Thiele, C., Dörr, K., Bilani, O., Rödel, J. & Schultz, L. Influence of strain on the magnetization and magnetoelectric effect in $La_{0.7}A_{0.3}MnO_3$/PMN-PT (001)(A= Sr, Ca). *Phys. Rev. B* **75**, 054408 (2007).
32. Biegalski, M. D., Doerr, K., Kim, D. H. & Christen, H. M. Applying uniform reversible strain to epitaxial oxide films. *Appl. Phys. Lett.* **96**, 151905 (2010).
33. Klein, L. *et al.* Anomalous spin scattering effects in the badly metallic itinerant ferromagnet $SrRuO_3$. *Phys. Rev. Lett.* **77**, 2774 (1996).
34. Wu, X., Foltyn, S., Dye, R., Coulter, Y. & Muenchausen, R. Properties of epitaxial $SrRuO_3$ thin films. *Appl. Phys. Lett.* **62**, 2434–2436 (1993).
35. Singh, D. J. Electronic and magnetic properties of the 4*d* itinerant ferromagnet $SrRuO_3$. *J. Appl. Phys.* **79**, 4818–4820 (1996).
36. Mazin, I. & Singh, D. J. Electronic structure and magnetism in Ru-based perovskites. *Phys. Rev. B* **56**, 2556 (1997).
37. Khalifah, P., Ohkubo, I., Christen, H. M. & Mandrus, D. Evolution of transport and magnetic properties near the ferromagnetic quantum critical point in the series $Ca_xSr_{1-x}RuO_3$. *Phys. Rev. B* **70**, 134426 (2004).
38. Grutter, A., Wong, F., Arenholz, E., Vailionis, A. & Suzuki, Y. Evidence of high-spin Ru and universal magnetic anisotropy in $SrRuO_3$ thin films. *Phys. Rev. B* **85**, 134429 (2012).
39. Middey, S., Mahadevan, P. & Sarma, D. Dependence of magnetism on $GdFeO_3$ distortion in the t_{2g} system $ARuO_3$ (A= Sr, Ca). *Phys. Rev. B* **83**, 014416 (2011).
40. Vailionis, A., Siemons, W. & Koster, G. Room temperature epitaxial stabilization of a tetragonal phase in $ARuO_3$ (A= Ca and Sr) thin films. *Appl. Phys. Lett.* **93**, 051909 (2008).
41. Lu, W. *et al.* Effect of oxygen vacancies on the electronic structure and transport properties of $SrRuO_3$ thin films. *J. Appl. Phys.* **113**, 17E125 (2013).

Acknowledgments

This work was supported by the National Basic Research Program of China (Nos. 2012CB932304 and 2014AA032904) and National Natural Science Foundation of China (Grant Nos. 11174130 and U1232210).

Author contributions

W.P.Z. and D.H.W. designed the experiments. W.P.Z., Q.L., Y.Q.X., Q.M.Z. and L.Y.L. carried out the magnetic and transport measurements. The date were collected by W.P.Z. Results were analyzed and interpreted by W.P.Z., D.H.W., Q.Q.C. and Y.W.D. The manuscript was written by W.P.Z. and D.H.W.

Additional information

Competing financial interests: The authors declare no competing financial interests.

How to cite this article: Zhou, W.P. *et al.* Electric field manipulation of magnetic and transport properties in $SrRuO_3/Pb(Mg_{1/3}Nb_{2/3})O_3$-$PbTiO_3$ heterostructure. *Sci. Rep.* **4**, 6991; DOI:10.1038/srep06991 (2014).